Research Journal of Pharmaceutical, Biological and Chemical Sciences

Electrochemical, Gravimetric and Monte Carlo Simulation Studies on the Interaction of 5,6-Dibenzyloxyindole on Mild Steel in 1 M HCl.

Toumiat K[1], EL Aoufir Y[2,3], Lgaz H[2,4], Salghi R[4*], Jodeh S[5], Zougagh M[6,7], and Oudda H[2].

[1]Department of Materials Sciences, Laghouat University, PO Box 37, 03000, Laghouat, Algeria.
[2]Laboratory of separation methods, Faculty of Science, Ibn Tofail University PO Box 242, Kenitra, Morocco.
[3]Laboratoire des matériaux, nanotechnologie et environnement.Université M[ed] V, Rabat, Morocco.
[4]Laboratory of Applied Chemistry and Environment, ENSA, Ibn Zohr University, PO Box 1136, 80000 Agadir, Morocco.
[5]Department of Chemistry, An-Najah National University, P. O. Box 7, Nablus, Palestine.
[6]Regional Institute for Applied Chemistry Research, IRICA, Ciudad Real, Spain.
[7]Albacete Science and Technology Park, E-02006, Albacete, Spain.

ABSTRACT

The inhibiting effect of 5,6-Dibenzyloxyindole (DPI) on corrosion of carbon steel (CS) was investigated in hydrochloric acid (1.0 M) by electrochemical and weight loss studies. It was found that DPI inhibits both partial corrosion reactions. The corrosion protection mechanism is by formation of a surface-adsorbed DPI film. A maximum inhibition efficiency of 93.03 % was achieved in 1.0 M HCl. The adsorption of DPI onto the CS surface was described by the Langmuir adsorption isotherm. The corresponding standard Gibbs energy of adsorption was calculated to be -36.84 kJ mol^{-1}. Monte Carlo simulation approach was used to ascertain the correlation between inhibitive effect and molecular structure. Both the experimental and theoretical studies agree well in this regard and confirm that DPI is having a better interaction with the metal surface in 1.0 M HCl. The adsorption behaviors of this molecule on the steel surface have been studied using Monte Carlo method.
Keywords: Corrosion inhibition, Mild steel, 5,6-Dibenzyloxyindole, Monte Carlo simulation, Hydrochloric acid

*Corresponding author

INTRODUCTION

From a materials standpoint, carbon steel is the most widely used engineering metal in marine applications, nuclear power and fossil fuel power plants, transportation, chemical processing, petroleum production, and refining, pipelines, mining, construction, processing equipment, motor vehicles, and household durables. However, one of the major problems related to its use is its low corrosion resistance in these environments[1–6]. A number of compounds are known to be applicable as corrosion inhibitors for carbon steel[7–13]. Such compounds typically contain nitrogen, oxygen, or sulfur in a conjugated system and function via adsorption of the molecules on the metal surface, creating a barrier to corrodent attack. An adsorption process between DPI and the steel surface was suggested. However, very little is known about the inhibition mechanism underlying the interaction of this compound with the metal surface elicited by adsorption. A description of this mechanism at the atomic level is currently lacking and deserves special attention[14–21]. In this regard, Monte Carlo simulation have been employed as a useful tool in corrosion inhibitor research[22–24]. Consequently, the research presented in this manuscript investigates the possibility of using 5,6-Dibenzyloxyindole (DPI), Fig. 1, as corrosion inhibitor for carbon steel in HCl solutions. The goal of the research was to determine the DPI corrosion inhibition efficiency and the mechanism of its corrosion inhibition using electrochemical, weight loss and Monte Carlo simulation studies.
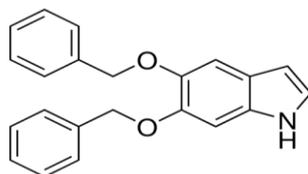

Figure 1. Chemical structure of tested compound.

MATERIALS AND METHODS

Electrodes, chemicals and test solution

Corrosion tests have been performed, using the gravimetric and electrochemical measurements, on electrodes cut from sheets of carbon steel with the chemical composition: 0.370 % C, 0.230 % Si, 0.680 % Mn, 0.016 % S, 0.077 % Cr, 0.011 % Ti, 0.059 % Ni, 0.009 % Co, 0.160 % Cu, and the remainder iron. The aggressive medium of molar hydrochloric acid used for all studies were prepared by dilution of analytical grade 37% HCl with double distilled water. The concentrations of DPI used in this investigates were varied from 1.10^{-4} to 5.10^{-3} M. The inhibitor molecule used in this paper was purchased from Sigma–Aldrich and have the structure presented in Fig. 1.

Gravimetric measurements

Gravimetric measurements were realized in a double walled glass cell equipped with a thermostat-cooling condenser. The carbon steel specimens used have a rectangular form with dimension of $2.5 \times 2.0 \times 0.2$ cm were abraded with a different grade of emery paper (320-800-1200) and then washed thoroughly with distilled water and acetone. After weighing accurately, the specimens were immersed in beakers which contained 100 ml acid solutions without and with various concentrations of DPI at temperature equal to 303 K remained by a water thermostat for 6h as immersion time. The gravimetric tests were performed by triplicate at same conditions.

The corrosion rates (C_R) and the inhibition efficiency ($\eta_{wt}\%$) of carbon steel have been evaluated from mass loss measurement using the following equations:

$$C_R = \frac{w}{St} \qquad (1)$$

$$\eta_{wt}\% = \frac{C_R^o - C_R}{C_R^o} \times 100 \qquad (2)$$

Where w is the average weight loss before and after exposure, respectively, S is the surface area of sample, t is the exposure time, C_R^o and C_R is the corrosion rates of steel without and with the DPI inhibitor, respectively.

Electrochemical tests

The potentiodynamic polarization curves were conducted using an electrochemical measurement system PGZ 100 Potentiostat/Galvanostat controlled by a PC supported by the Voltamaster 4.0 Software. The electrochemical measurements were performed in a conventional three electrode glass cell with carbon steel as a working electrode, platinum as counter electrode (Pt) and a saturated calomel electrode used as a reference electrode. The working electrode surface was prepared as described above gravimetric section. Prior to each electrochemical test an immersion time of 30 min was given to allow the stabilization system at corrosion potential. The polarization curves were obtained by changing the electrode potential automatically from -800 to -200 mV/SCE at a scan rate of 1 mV s-1. The temperature is thermostatically controlled at desired temperature ±1K.The percentage protection efficiency (η_P %) is defined as:

$$\eta_{PDP}(\%) = \frac{I_{corr}^0 - I_{corr}}{I_{corr}^0} x\ 100 \qquad (3)$$

Where, I_{corr}^o are corrosion current in the absence of inhibitor, Icorr are corrosion current in the presence of inhibitor.

Electrochemical impedance spectroscopy (*EIS*) measurements were carried out with same equipment used for potentiodynamic polarization study (Voltalab PGZ 100) at applied sinusoidal potential waves of 5mV amplitudes with frequencies ranging from 100 KHz to 10 mHz at corrosion potential. The impedance diagrams are given in the Nyquist representation. The charge transfer resistance (R_{ct}) was determined from Nyquist plots and double layer capacitance (C_{dl}) was calculated from *CPE* parameters of the equivalent circuit deduced using Zview software. In this case the percentage protection efficiency (η_{EIS}%) is can be calculated by the value of the charge transfer resistance (R_{ct})

$$\eta_{EIS}(\%) = \frac{R_{ct} - R_{ct}^0}{R_{ct}} x\ 100 \qquad (4)$$

Where R_{ct}^o and Rct were the polarization resistance of uninhibited and inhibited solutions, respectively.

Monte Carlo simulation study

The Monte Carlo (MC) search was adopted to compute the low configuration adsorption energy of the interactions of the DPI on a clean iron surface. The Monte Carlo (MC) simulation was carried out using Materials Studio 6.0 software (Accelrys, Inc.)[25]. The Fe crystal was cleaved along the (1 1 0) plane, it is the most stable surface as reported in the literature. Then, the Fe (1 1 0) plane was enlarged to (10x10) supercell to provide a large surface for the interaction of the inhibitor. The simulation of the interaction between DPI and the Fe (1 1 0) surface was carried out in a simulation box (24.82 × 24.82 × 30.13 Å) with periodic boundary conditions, which modeled a representative part of the interface devoid of any arbitrary boundary effects. After that, a vacuum slab with 30 Å thickness was built above the Fe (1 1 0) plane. All simulations were implemented with the COMPASS force field to optimize the structures of all components of the system of interest[26]. More simulation details on the methodology of Monte Carlo simulations can be found in previous publications[22,24]

RESULTS AND DISCUSSION

Weight loss study

Table 1 presented weight loss, corrosion rate and inhibition efficiency in the absence and presence of different concentrations of DPI. It followed from Table 1 that the weight loss decreased (i.e., corrosion rate is suppressed), and therefore the corrosion inhibition strengthened, with increase in inhibitor concentration. This

trend may result from the fact that adsorption and surface coverage increased with the increase in DPI concentration.

Table 1: Inhibition efficiency of various concentrations of DPI for corrosion of MS in 1M HCl obtained by weight loss measurements at 303K.

Inhibitors	Concentration (M)	C_R (mg cm^{-2} h^{-1})	η_w (%)	Θ
Blank	1.0	1.135	-	-
DPI	5.10^{-3}	0.0903	92.04	0.9204
	1.10^{-3}	0.1201	89.42	0.8942
	5.10^{-4}	0.1391	87.74	0.8774
	1.10^{-4}	0.1824	83.93	0.8393

Polarization results

Polarization measurements were carried out in order to gain knowledge concerning the kinetics of the cathodic and anodic reactions. Fig. 2 presented the results of the effect of DPI concentration on the cathodic and anodic polarization curves of mild steel in 1 M HCl. It could be observed that both the cathodic and anodic reactions were suppressed with the addition of DPI, which suggested that the DPI reduced anodic dissolution and retarded the hydrogen evolution reaction[27].
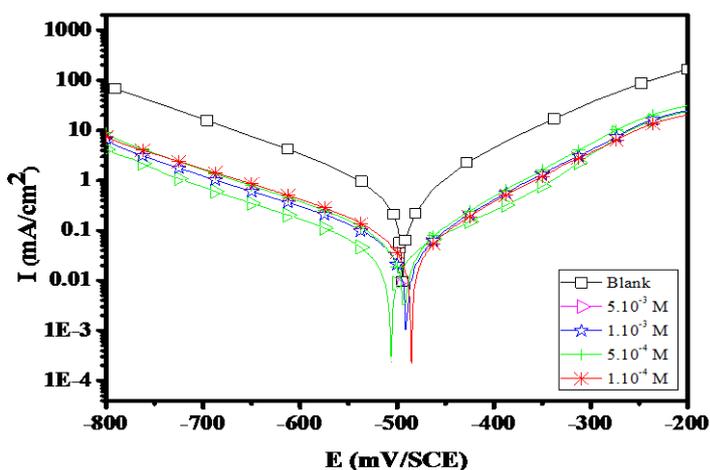

Figure 2. Polarisation curves of MS in 1 M HCl for various concentrations of DPI at 303K.

Electrochemical corrosion kinetics parameters, i.e., corrosion potential (E_{corr}), cathodic Tafel slope (βc) and corrosion current density (i_{corr}) obtained from the extrapolation of the polarization curves, were given in Table 2.

Table 2: Corrosion parameters for corrosion of MS with selected concentrations of DPI in 1M HCl by *PDP* method at 303K.

Inhibitor	Concentration (M)	$-E_{corr}$ (mV/SCE)	$-\beta c$ (mV dec^{-1})	i_{corr} (µA cm^{-2})	η_{Tafel} (%)	Θ
Blank	-	496	162.0	564.0	-	-
DPI	5.10^{-3}	508.2	157.9	42.4	92.48	0.9248
	1.10^{-3}	493.5	165.7	65.3	88.42	0.8842
	5.10^{-4}	494.3	155.8	75.1	86.68	0.8668
	1.10^{-4}	488.4	167.9	88.8	84.25	0.8425

It can be seen from Table 2 that both cathodic and anodic reactions of mild steel were inhibited with the increase in concentrations of the studied compounds in 1.0 M HCl. No systematic variation either only in

anodic or cathodic direction can be seen in E_{corr} values depending on inhibitor concentrations, and accordingly, the measure of variation is insignificant. Based on these data, it can be said that this compound is mixed-type inhibitor and inhibit corrosion by blocking the active sites of the metal[27,28]. The increase in the inhibition efficiencies with the increase in the concentrations of the studied inhibitor shows that the inhibitory actions may be due to the adsorption of the inhibitor on steel surface.

EIS study

Impedance method provides information about the kinetics of the electrode processes and simultaneously about the surface properties of the investigated systems[29,30]. The shape of impedance gives mechanistic information (Table 3). The method is widely used for investigation of the corrosion inhibition processes. Fig. 3 shows the *EIS* spectra of the CS electrode recorded in the absence and presence of DPI at different concentrations. The spectra were recorded at 303 K after the stabilization of the electrode at OCP for 0.5 h.
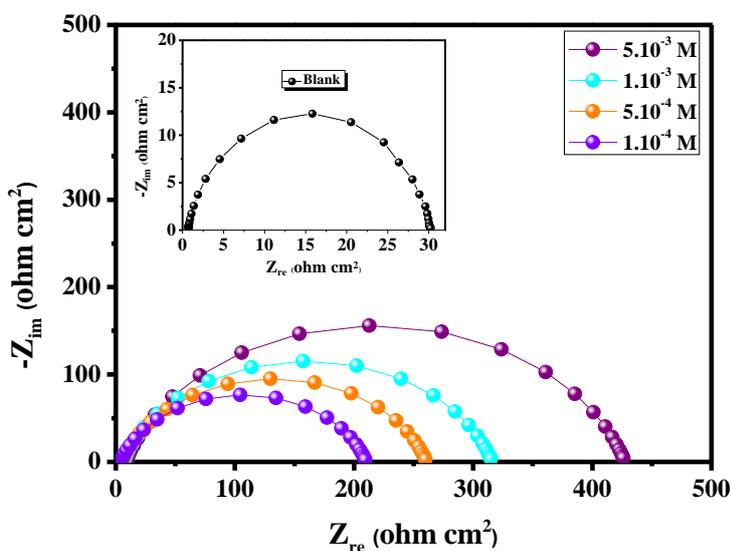

Figure 3. Nyquist curves for mild steel in 1 M HCl for selected concentrations of DPI at 303K.

The figure shows that the diameter of the semicircle increases with the increase in inhibitor concentration in the electrolyte, indicating an increase in corrosion resistance of the material[8,14]. In order to extract qualitative information, the impedance spectra were fitted to the $Rs(R_{ct}CPE)$ equivalent circuit of the form in Fig. 4. Where Rs is the solution resistance, R_{ct} denotes the charge-transfer resistance and CPE is constant phase element. The introduction of CPE into the circuit was necessitated to explain the depression of the capacitance semicircle, which corresponds to surface heterogeneity resulting from surface roughness, impurities, and adsorption of inhibitors[3,20].

Figure 4. Equivalent electrical circuit.

The impedance of this element is frequency-dependent and can be calculated using the Eq. 5[27]:

$$Z_{CPE} = \frac{1}{Q(j\omega)^n}$$

(5)

Where Q is the *CPE* constant (in Ω^{-1} S^n cm^{-2}), ω is the angular frequency (in rad s^{-1}), $j^2 = -1$ is the imaginary number and n is a *CPE* exponent which can be used as a gauge for the heterogeneity or roughness of the surface[28]. In addition, the double layer capacitances, C_{dl}, for a circuit including a *CPE* were calculated by using the following Eq. 6:

$$C_{dl} = \left(Q.R_{ct}^{1-n}\right)^{1/n}$$

(6)

The double layer between charged metal surface and the solution is considered as an electrical double capacitor. The adsorption of indole derivative on the mild steel decreases its electrical capacity (Table 3) because they displace the water molecule and other ions originally adsorbed on the metal surface[27]. The decrease in this capacity with increase in concentration of the inhibitor may be attributed to the formation of a protective film on the electrode surface. The thickness of this protective layer also increases with increase in inhibitor concentration as more inhibitor adsorbed on the electrode surface, resulting in a noticeable decrease in C_{dl}[29,30].

Table 3: AC-impedance parameters for corrosion of mild steel for selected concentrations of DPI in 1M HCl at 303K.

Inhibitor	Concentration (M)	R_{ct} (Ω cm^2)	n	$Q \times 10^{-4}$ (s^n Ω^{-1}cm^{-2})	C_{dl} (μF cm^{-2})	η_{EIS} (%)	Θ
Blank	1.0	29 .35	0.910	1.7610	91.6	-	-
DPI	5.10^{-3}	421.01	0.893	0.1398	7.55	93.03	0.9303
	1.10^{-3}	309.6	0.882	0.2468	12.85	90.52	0.9052
	5.10^{-4}	255.6	0.862	0.3996	19.18	88.52	0.8852
	1.10^{-4}	205.9	0.839	0.7194	32.05	85.74	0.8574

Adsorption isotherm

It is clear from the *EIS* measurements that DPI adsorbs on the CS surface and in that way inhibits general corrosion of the surface, by forming a mass-transfer barrier for solvated corrosive ions. Therefore, it would be quite useful to describe the adsorption process by an appropriate adsorption isotherm, which could provide further useful insights into the interaction of the inhibitor and the metal surface and on the mechanism of corrosion inhibition. In 1 M HCl, DPI adsorption follows the Langmuir isotherm (Fig. 5) as per Eq.7[31]:

$$\frac{C}{\theta} = \frac{1}{K_{ads}} + C$$

(7)

Where, C is the concentration of the inhibitor, K_{ads} is the equilibrium constant of adsorption and ϑ is the surface coverage. The Langmuir approach is based on a molecular kinetic model of the adsorption–desorption process. On the other hand, the adsorption equilibrium constant (K_{ads}) is related to the standard free energy of adsorption ($\Delta G°_{ads}$) of the inhibitor molecules by the following Eq. 8[32]:

$$K_{ads} = \frac{1}{55.5}\exp\left(\frac{-\Delta G^0_{ads}}{RT}\right)$$

(8)

Where R is the universal gas constant, T the absolute temperature in K, and 55.5 represents the molar concentration of water in the solution.
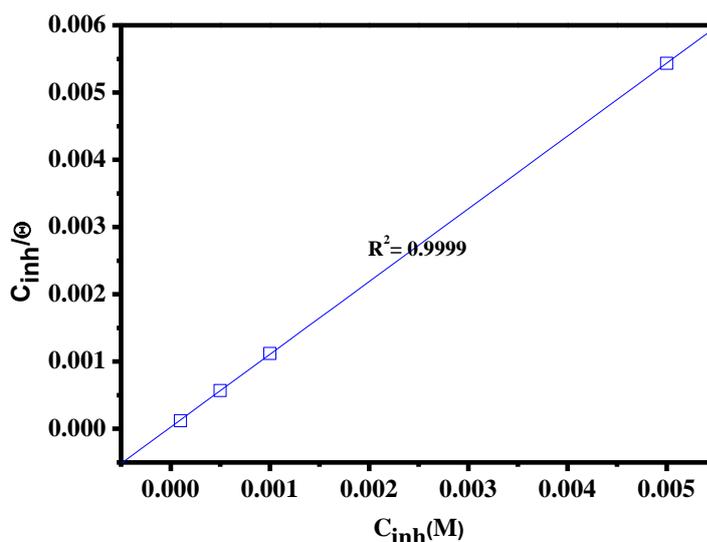
Figure 5: Langmuir adsorption of inhibitor on the MS surface in 1.0 M HCl solution at 303K.

Adsorption of inhibitor involves the formation of two types of interaction responsible for bonding of inhibitor to a metal surface. The first one (physical adsorption) is weak undirected interaction and is due to electrostatic attraction between inhibiting organic ions or dipoles and the electrically charged surface of metal. The second type of interaction (adsorption) occurs when directed forces govern the interaction between the adsorbate and adsorbent. Chemical adsorption involves charge sharing or charge transfer from adsorbates to the metal surface atoms in order to form a coordinate type of bond. Chemical adsorption has a free energy of adsorption and activation energy higher than physical adsorption and, hence, usually it is irreversible[33–35]. Values of the free energy calculated from Eq. (8) are recorded in Table 4. From the result obtained, the free energy is found to be -36.84 kJ/mol. Therefore, the adsorption of DPI on mild steel surface is consistent with both electrostatic and charge sharing from the inhibitor molecule to Fe in mild steel and supports physical and chemical adsorption[34,35].

Table 4: Adsorption parameters of inhibitor for MS corrosion in 1M HCl at 303 K

Inhibitor	Slope	K_{ads}(M^{-1})	ΔG°_{ads} (kJ/mol)
DPI	1.08	40790	-36.84

Molecular dynamic (Monte Carlo) simulation

Monte Carlo simulation were performed on a system comprising DPI molecule and iron surface. An adsorption calculation was done on DPI/iron to find the lowest energy for the whole system[23]. The outputs and descriptors are presented in Table 5. The parameters presented in Table 5 included total energy, in kcal mol^{-1}, of the substrate–adsorbate configuration. The total energy is defined as the sum of the energies of the adsorbate components, the rigid adsorption energy, and the deformation energy. In this study, adsorption energy in kcal mol^{-1}, reports energy released (or required) when the relaxed adsorbate components are adsorbed on the substrate. Table 5 shows also (dEads/dNi), which reports the energy, in kcal mol-1, of substrate–adsorbate configurations where one of the adsorbate components has been removed[36]. As can be seen from Table 5, the adsorption energy during the simulation process for DPI molecule are negative and highest -198.810 Kcal/mol). High values of adsorption energy indicate that DPI molecule will give the highest inhibition efficiency[22,24]. The shape of DPI molecules on iron surface is shown in Figure 6.
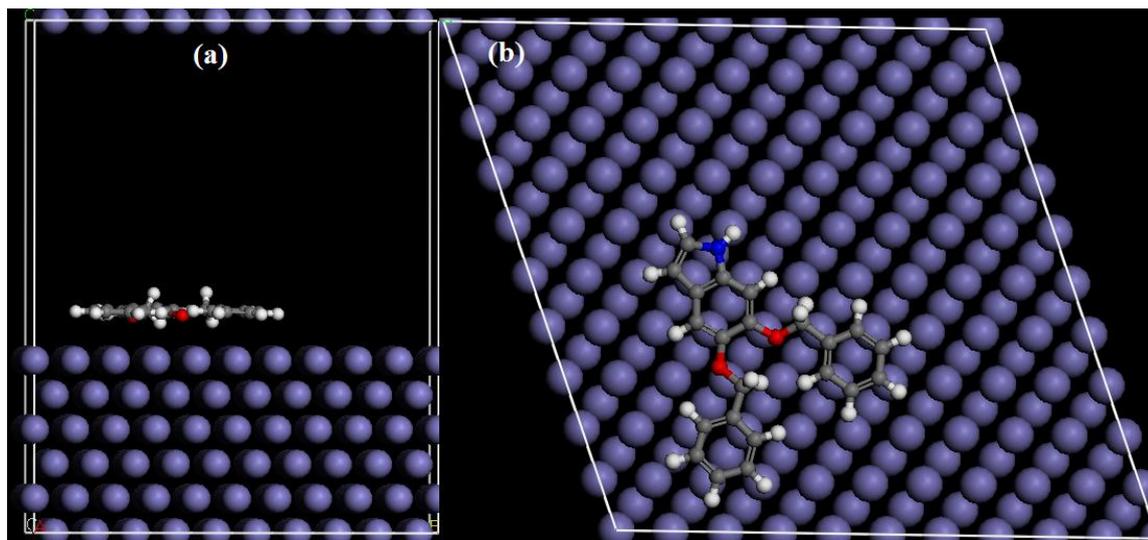
Figure 6. The most stable low energy configuration for the adsorption of the inhibitor on Fe (1 1 0) surface obtained through the Monte Carlo simulation.(a) side view, (b) top view.

Table 5. Outputs and descriptors calculated by the Monte Carlo simulation for the lowest adsorption. Configurations of DPI Fe (1 1 0) surface (in kcal/mol).

System	Total energy	Adsorption energy	Rigid adsorption energy	Deformation energy	dEad/dNi inhibitor
Fe (1 1 0)/DPI	-16.528	-198.810	-194.501	-4.309	-198.810

CONCLUSION

From the above study it is concluded that 5-(Benzyloxy)indole (DPI) exhibited good inhibition efficiency on mild steel in 1 M HCl. The inhibition efficiency increases on increasing DPI concentration and maximum value was obtained at 5.10^{-3} M concentration. The adsorption of DPI on mild steel surface obeys the Langmuir adsorption isotherm. Potentiodynamic polarization study shows that studied DPI is a mixed type inhibitor. *EIS* study shows that the DPI forms a protective surface film on metal/electrolyte interface. The molecular dynamics simulations study supports the weight loss and electrochemical measurements and indicate that there is strong interaction between mild steel and the DPI.

ACKNOWLEDGEMENTS

REFERENCES

[1] Adardour L, Larouj M, Lgaz H, Belkhaouda M, Salghi R, Jodeh S, et al. Pharma Chem 2016;8:152–60.
[2] Adardour L, Lgaz H, Salghi R, Larouj M, Jodeh S, Zougagh M, et al. Pharm Lett 2016;8:212–24.
[3] Adardour L, Lgaz H, Salghi R, Larouj M, Jodeh S, Zougagh M, et al. Pharm Lett 2016;8:173–85.
[4] Adardour L, Lgaz H, Salghi R, Larouj M, Jodeh S, Zougagh M, et al. Pharm Lett 2016;8:126–37.
[5] Afia L, Larouj M, Lgaz H, Salghi R, Jodeh S, Samhan S, et al. Pharma Chem 2016;8:22–35.
[6] Afia L, Larouj M, Salghi R, Jodeh S, Zougagh M, Rasem Hasan A, et al. Pharma Chem 2016;8:166–79.
[7] Bousskri A, Salghi R, Anejjar A, Jodeh S, Quraishi MA, Larouj M, et al. Chem 2016;8:67–83.
[8] El Makrini B, Larouj M, Lgaz H, Salghi R, Salman A, Belkhaouda M, et al. Pharma Chem 2016;8:227–37.
[9] El Makrini B, Lgaz H, Larouj M, Salghi R, Rasem Hasan A, Belkhaouda M, et al. Pharma Chem 2016;8:256–68.
[10] Larouj M, Belkhaouda M, Lgaz H, Salghi R, Jodeh S, Samhan S, et al. Pharma Chem 2016;8:114–33.
[11] Larouj M, Lgaz H, Salghi R, Jodeh S, Messali M, Zougagh M, et al. Mor J Chem 2016;4:567–83.

[12]   Larouj M, Lgaz H, Salghi R, Oudda H, Jodeh S, Chetouani A. Mor J Chem 2016;4:425–36.
[13]   Larouj M, Lgaz H, Houda S, Zarrok H, Zarrouk A, Elmidaoui A, et al. J Mater Environ Sci 2015;6:3251–67.
[14]   Lgaz H, Anejjar A, Salghi R, Jodeh S, Zougagh M, Warad I, et al. Int J Corros Scale Inhib 2016;5:209–231.
[15]   Lgaz H, Benali O, Salghi R, Jodeh S, Larouj M, Hamed O, et al. Pharma Chem 2016;8:172–90.
[16]   Lgaz H, ELaoufir Y, Ramli Y, Larouj M, Zarrok H, Salghi R, et al. Pharma Chem 2015;7:36–45.
[17]   Lgaz H, Salghi R, Larouj M, Elfaydy M, Jodeh S, Abbout H, et al. Mor J Chem 2016;4:592–612.
[18]   Lgaz H, Belkhaouda M, Larouj M, Salghi R, Jodeh S, Warad I, et al. Mor J Chem 2016;4:101–11.
[19]   Lotfi N, Lgaz H, Belkhaouda M, Larouj M, Salghi R, Jodeh S, et al. Arab J Chem Environ Res 2015;1:13–23.
[20]   Saadouni M, Larouj M, Salghi R, Lgaz H, Jodeh S, Zougagh M, et al. Pharm Lett 2016;8:65–76.
[21]   Saadouni M, Larouj M, Salghi R, Lgaz H, Jodeh S, Zougagh M, et al. Pharm Lett 2016;8:96–107.
[22]   Eivani AR, Zhou J, Duszczyk J. Comput Mater Sci 2012;54:370–7. doi:10.1016/j.commatsci.2011.10.016.
[23]   Kaya S, Tüzün B, Kaya C, Obot IB. J Taiwan Inst Chem Eng 2016;58:528–35. doi:10.1016/j.jtice.2015.06.009.
[24]   Khaled KF, El-Maghraby A. Arab J Chem 2014;7:319–26. doi:10.1016/j.arabjc.2010.11.005.
[25]   Materials Studio. Revision 6.0. Accelrys Inc., San Diego, USA; 2013.
[26]   Sun H. J Phys Chem B 1998;102:7338–64.
[27]   Yadav M, Kumar S, Bahadur I, Ramjugernath D. Int J Electrochem Sci 2014;9:3928–50.
[28]   Yadav M, Behera D, Kumar S. Surf Interface Anal 2014;46:640–52.
[29]   Hmamou DB, Salghi R, Zarrouk A, Zarrok H, Touzani R, Hammouti B, et al. J Environ Chem Eng 2015;3:2031–41. doi:10.1016/j.jece.2015.03.018.
[30]   Bammou L, Belkhaouda M, Salghi R, Benali O, Zarrouk A, Zarrok H, et al. J Assoc Arab Univ Basic Appl Sci 2014;16:83–90. doi:10.1016/j.jaubas.2013.11.001.
[31]   Bentiss F, Lebrini M, Lagrenée M. Corros Sci 2005;47:2915–31.
[32]   Bentiss F, Lebrini M, Lagrenée M. Corros Sci 2005;47:2915–31.
[33]   Yadav M, Sinha R, Kumar S, Sarkar T. RSC Adv 2015;5:70832–48.
[34]   Yadav DK, Maiti B, Quraishi M. Corros Sci 2010;52:3586–98.
[35]   Verma C, Quraishi MA, Olasunkanmi LO, Ebenso EE. RSC Adv 2015;5:85417–30. doi:10.1039/C5RA16982H.
[36]   Obot IB, Kaya S, Kaya C, Tüzün B. Phys E Low-Dimens Syst Nanostructures n.d. doi:10.1016/j.physe.2016.01.024.